ORIGINAL ARTICLE

Mucins MUC5AC and MUC5B Are Variably Packaged in the Same and in Separate Secretory Granules

Oanh N. Hoang[1]*, Anna Ermund[2]*, Ana M. Jaramillo[1]*, Dalia Fakih[2], Cory B. French[3], Jose R. Flores[3], Harry Karmouty-Quintana[4], Jesper M. Magnusson[2], Giorgio Fois[5], Michael Fauler[5], Manfred Frick[5], Peter Braubach[6], Joshua B. Hales[3], Richard C. Kurten[7], Reynold Panettieri[8], Leoncio Vergara[9], Camille Ehre[10], Roberto Adachi[1], Michael J. Tuvim[1]*, Gunnar C. Hansson[2]*, and Burton F. Dickey[1]*

[1]Department of Pulmonary Medicine, The University of Texas MD Anderson Cancer Center, Houston, Texas; [2]Department of Medical Biochemistry and Cell Biology, University of Gothenburg, Gothenburg, Sweden; [3]Washington University School of Medicine, St. Louis, Missouri; [4]Division of Critical Care, Pulmonary, and Sleep Medicine, Department of Biochemistry and Molecular Biology, University of Texas Health Science Center at Houston, Houston, Texas; [5]Institute of General Physiology, Ulm University, Ulm, Germany; [6]Hannover Medical School Hospital, Hannover, Germany; [7]University of Arkansas for Medical Sciences, Little Rock, Arkansas; [8]Rutgers New Jersey Medical School, New Brunswick, New Jersey; [9]Institute of Biosciences and Technology, Texas A&M School of Medicine, Houston, Texas; and [10]Marsico Lung Institute, University of North Carolina at Chapel Hill, Chapel Hill, North Carolina

ORCID IDs: 0000-0001-5304-585X (O.N.H.); 0000-0002-3233-043X (A.E.); 0000-0001-8089-4275 (A.M.J.); 0000-0003-1655-3614 (C.B.F.); 0000-0003-2942-6147 (J.R.F.); 0000-0003-4753-9823 (H.K.-Q.); 0000-0002-5630-0155 (J.M.M.); 0000-0001-5414-1149 (G.F.); 0000-0002-7371-849X (M. Fauler); 0000-0002-4763-1104 (M. Frick); 0000-0003-3673-7779 (P.B.); 0000-0003-1122-3990 (J.B.H.); 0000-0003-0834-4636 (R.P.); 0000-0001-7427-9567 (L.V.); 0000-0002-0046-0096 (C.E.); 0000-0002-0146-0768 (R.A.); 0000-0001-8126-7716 (M.J.T.); 0000-0002-1900-1869 (G.C.H.); 0000-0002-4780-1847 (B.F.D.).

Abstract

Rationale: MUC5AC (mucin 5AC, oligomeric gel-forming) and MUC5B (mucin 5B, oligomeric gel-forming) are the predominant secreted polymeric mucins in mammalian airways. They contribute differently to the pathogenesis of various muco-obstructive and interstitial lung diseases, and their genes are separately regulated, but whether they are packaged together or in separate secretory granules is not known.

Objectives: To determine the packaging of MUC5AC and MUC5B within individual secretory granules in mouse and human airways under varying conditions of inflammation and along the proximal–distal axis.

Methods: Lung tissue was obtained from mice stimulated to upregulate mucin production by the cytokines IL-1β and IL-13 or by porcine pancreatic elastase. Human lung tissue was obtained from donated normal lungs, biopsy samples of transplanted lungs, and explanted lungs from subjects with chronic obstructive pulmonary disease. MUC5AC and MUC5B were labeled with antibodies from different animal species or, in mice only, by transgenic chimeric mucin-fluorescent proteins and imaged using widefield deconvolution or Airyscan fluorescence microscopy.

Measurements and Main Results: In both mouse and human airways, most secretory granules contained both mucins interdigitating within the granules. Smaller numbers of granules contained MUC5B alone, and even fewer contained MUC5AC alone.

Conclusions: MUC5AC and MUC5B are variably stored both in the same and in separate secretory granules of both mice and humans. The high fraction of granules containing both mucins under a variety of conditions makes it unlikely that their secretion can be differentially controlled as a therapeutic strategy. This work also advances knowledge of the packaging of mucins within secretory granules to understand mechanisms of epithelial stress in the pathogenesis of chronic lung diseases.

Keywords: airway mucins; MUC5AC; MUC5B; mucus; club cells

(Received in original form February 15, 2022; accepted in final form July 1, 2022)

*These authors contributed equally to this work.

Correspondence and requests for reprints should be addressed to Burton F. Dickey, M.D., Department of Pulmonary Medicine, Unit 1059, The University of Texas MD Anderson Cancer Center, 1515 Holcombe Boulevard, Houston, TX 77030. E-mail: bdickey@mdanderson.org.

This article has a related editorial.

This article has an online supplement, which is accessible from this issue's table of contents at www.atsjournals.org.

Am J Respir Crit Care Med Vol 206, Iss 9, pp 1081–1095, Nov 1, 2022

Originally Published in Press as DOI: 10.1164/rccm.202202-0309OC on July 1, 2022
Internet address: www.atsjournals.org

At a Glance Commentary

Scientific Knowledge on the Subject: The two major airway mucins, MUC5AC (mucin 5AC, oligomeric gel-forming) and MUC5B (mucin 5B, oligomeric gel-forming), have distinct physical properties and functions despite similarity in structure. MUC5AC is important for protection against helminth migration through the lungs but disproportionally contributes to formation of mucus plaques in allergic airway inflammation. MUC5B is important for homeostatic mucociliary clearance, but a high-expressing allele contributes to idiopathic pulmonary fibrosis. Both mucins can be produced within a single surface airway secretory cell, but whether they are packaged together within individual secretory granules is not known.

What This Study Adds to the Field: Using high-resolution light microscopy of mouse and human tissues, we find that in cells producing both mucins, most granules contain both mucins. This finding suggests that therapeutic strategies to differentially modulate secretion of either MUC5AC or MUC5B will not be effective. In addition, we find that the two mucins interdigitate within granules, which might have implications for protein homeostasis and cellular stress in chronic lung diseases.

Mucus forms a mobile barrier in the conducting airways, trapping inhaled pathogens, particles, and toxicants, which are then propelled out of the lungs by ciliary beating (1, 2). Mucus is formed by the interactions of secreted polymeric mucins with water and ions, resulting in a gel-like substance that has variable viscoelastic and lubricant versus adhesive properties depending on its hydration status (3, 4). The secreted mucins are very large, highly glycosylated proteins that polymerize into linear chains and networks. Two polymeric mucins are secreted into the airways, MUC5AC (mucin 5AC, oligomeric gel-forming) and MUC5B (mucin 5B, oligomeric gel-forming), with little or no contribution from other polymeric mucins (1, 5, 6).

Airway mucus is often considered a homogeneous mixture of MUC5AC and MUC5B, perhaps because of the clear, colorless, and homogeneous macroscopic appearance of normal mucus and perhaps because of similarities in the primary structure of MUC5AC and MUC5B (1, 3). However, recent work using immunohistochemical techniques shows that the two polymeric mucins can occupy distinct microscopic domains in airway mucus (7–10). In addition, MUC5B forms ~27-μm-diameter bundled strands that emanate from submucosal glands, while MUC5AC and MUC5B together form <2-μm-diameter threads that emanate from surface epithelial cells, with both elongated structures helping clear large particles (10–14). Despite similarities in their primary structure, genetic deletion experiments in mice have shown the two mucins to have distinct functions as follows. MUC5AC is required for the clearance of parasitic worms from the gut (15), and it traps migrating worms in the lungs (16, 17). MUC5B is required for ciliary clearance of microbes and particles, such that many MUC5B knockout mice die of infection and airway obstruction (18), and humans lacking MUC5B experience repeated lung infections and develop bronchiectasis (19). Pathologically, MUC5AC causes airflow obstruction in allergic asthma (20), an overexpressing allele of MUC5B is highly associated with interstitial lung disease (21, 22), and both mucins contribute to mucus dysfunction in cystic fibrosis (11, 23).

Our current understanding of mucus formation is further complicated by the recent recognition that baseline and stimulated mucin secretion are mediated by two different molecular machines (24). Both machines are variants of the conventional vesicle trafficking SNARE (soluble *N*-ethylmaleimide–sensitive factor attachment protein receptor) apparatus that has been conserved from yeast to man. However, although some molecular components are shared between the baseline and stimulated exocytic machines, such as SNAP23 (synaptosome associated protein 23) and Munc13-2 (mammalian uncoordinated 13-2) (25, 26), others are distinct, such as Munc18b (mammalian uncoordinated 18b), which functions predominantly in stimulated secretion, while Munc18a (mammalian uncoordinated 18a) functions in baseline secretion (27). The fast exocytic calcium sensor Syt2 (synaptotagmin 2) functions exclusively in stimulated secretion (28, 29).

MUC5AC and MUC5B are often synthesized and secreted within the same cells of the surface airway epithelium (1, 25, 30, 31). However, it is not known whether they are packaged into separate secretory granules or copackaged into a single population of granules. This question has important implications for the possible differential secretion of MUC5AC and MUC5B, for their interaction to form extracellular mucus, and for the induction of protein homeostasis (proteostasis) stress during their intracellular trafficking. To address this knowledge gap, we assembled panels of mucin-specific antibodies and transgenic fluorescent reporter mice, and performed high-resolution imaging studies of mouse and human airways. Some of the results of these studies have been previously reported in the form of an abstract (32).

Supported by NIH grants R01 HL129795 (B.F.D.), R01 HL138510 and R01 HL157100 (H.K.-Q.), UL1TR003017 (R.P.), and U01 AI095473 (G.C.H.); Cystic Fibrosis Foundation grants DICKEY18G0 (B.F.D.), DICKEY19P0 (B.F.D.), JARAMI20F0 (A.M.J.), and EHRE20XX0 (C.E.); the MD Anderson First Year Medical Student Program (C.B.F.); Deutsche Forschungsgemeinschaft grant 175083951 and the Boehringer Ingelheim Ulm University BioCenter (M. Frick); H2020 European Research Council grant 694181, Forskningsrådet om Hälsa, Arbetsliv och Välfärd grant 2017-00958 (J.M.M.); IngaBritt and Arne Lundberg Foundation grant 2018-0117 (G.C.H.); The Swedish Heart and Lung Foundation grants 20160241, 20190311, and 20200680 (A.E., G.C.H.); and the Swedish Cystic Fibrosis Foundation (A.E.).

Author Contributions: O.N.H., A.E., A.M.J., C.B.F., M.J.T., G.C.H., and B.F.D. conceived the research; O.N.H., A.E., A.M.J., D.F., J.M.M., C.B.F., J.R.F., G.F., and J.B.H. performed experiments; H.K.-Q., J.M.M., P.B., R.C.K., and R.P. supplied human tissue; C.E. supplied mucin antibodies; R.A. designed the object-based colocalization analysis of instance segmentation by thresholding and oversaw all statistical analyses at MD Anderson, and M. Fauler designed a similar object-based colocalization analysis for use at Ulm University; O.N.H., A.E., A.M.J., G.F., M. Frick, L.V., R.A., M.J.T., G.C.H., and B.F.D. analyzed data and interpreted results; O.N.H., A.E., A.M.J., M.J.T., and B.F.D. prepared figures; O.N.H., A.E., A.M.J., G.C.H., and B.F.D. drafted the manuscript; all authors edited and revised the manuscript, and all authors approved the final version.

Methods

Briefly, wild-type C57BL/6 mice, challenged with cytokines or elastase to induce mucous metaplasia, were studied at MD Anderson Cancer Center and the University of Gothenburg under approved institutional protocols. EGFP (enhanced green fluorescent protein)–MUC5B and mCherry-MUC5AC double-transgenic reporter mice were generated at the University of Gothenburg. Normal human tissue was obtained at the University of Texas Health Science Center at Houston, bronchial biopsy samples of airways of human subjects who had undergone lung transplantation were obtained at the University of Gothenburg, and lung explants and surgical biopsy samples of human subjects were obtained at Hannover Medical School Hospital, all under approved institutional protocols. For microscopic analysis, widefield deconvolution immunofluorescence microscopy was performed at MD Anderson Cancer Center and Airyscan (Zeiss) high-resolution microscopy at the University of Gothenburg. Detailed methods are provided in the online supplement.

Results

Mucin Expression in Mouse Airway Secretory Cells in Response to IL-1β or IL-13

In naive mouse airways, MUC5B is produced constitutively in secretory cells from the trachea to preterminal bronchioles and is readily detectable by immunohistochemical staining (25, 30, 33). However, MUC5AC is nearly undetectable (20, 33), so we stimulated MUC5AC production with cytokines delivered by intrapharyngeal instillation. With a high degree of mucous metaplasia, cells are so densely packed with mucin granules that resolving individual granules by light microscopy is difficult (27, 30). Therefore, we induced a low degree of metaplasia in the left axial bronchus using two cytokines, IL-1β and IL-13, which are prominently elevated in cystic fibrosis and asthma, respectively (27, 34). Increased mucin production is illustrated in Figures 1A and 1B and analyzed in the Results section of the online supplement.

To determine the expression of each mucin within individual secretory cells of the axial bronchus, MUC5AC and MUC5B were immunolabeled and imaged using fluorescence microscopy (Figure 1C). After low-dose stimulation with IL-1β, approximately half of cells contained MUC5B alone and half contained both MUC5B and MUC5AC, but virtually no cells contained MUC5AC alone (Figure 1C). After low-dose stimulation with IL-13, most cells (74%) contained both mucins, while 22% contained MUC5B alone and 4% contained MUC5AC alone.

Colocalization of MUC5AC and MUC5B within Mucin Granules in Mouse Airways Stimulated with IL-1β or IL-13

For mucin colocalization analysis within secretory granules by immunofluorescence microscopy, we focused on cells expressing both mucins and observed three types of granules in response to either cytokine: granules containing MUC5AC only, MUC5B only, or both mucins. For granules that appeared to contain both mucins in low-resolution images (Figure 1C), we sought certainty that the fluorophores were contained within a single granule rather than in separate, closely apposed, granules. This was achieved by using high-resolution widefield microscopy with postacquisition deconvolution of the images. Circular areas filled by the two fluorophores were observed, consistent with spherical granules densely packed with mucins (Figure 2). This spatial arrangement was particularly apparent in large granules $\sim$1 μm in diameter, and the two mucins were seen to interdigitate rather than to be segregated into distinct domains (Figures 2B and 2D). No differences were apparent between IL-1β and IL-13 in the spatial arrangement of the two mucins within granules.

Quantification of Mucin Granule Populations in Mouse Airways Stimulated with IL-1β or IL-13

To quantify the colocalization of MUC5AC and MUC5B within secretory granules across numerous cells of mouse axial bronchi imaged by widefield deconvolution immunofluorescence microscopy, we first used a global statistical approach by performing Pearson's correlation coefficient (PCC) and Mander's colocalization coefficient (MCC) analyses. For IL-1β, PCC was 0.75 (*see* Figure E2A in the online supplement), consistent with localization of the two mucins both within the same granules and within separate granules. MCC analysis similarly showed MUC5AC red fluorescence present to a high degree in $MUC5B^+$ green pixels (M1 = 0.68) and MUC5B green fluorescence present to a high degree in $MUC5AC^+$ red pixels (M2 = 0.74) (*see* Figure E2A). For IL-13, PCC (0.65) and MCC (M1 = 0.57, M2 = 0.70) analyses similarly showed a high degree of colocalization of the two fluorophores (*see* Figure E2B). When the fluorophores of the secondary antibodies were switched, there was no significant difference in PCC or MCC (not shown).

We then used an object-based approach of instance segmentation by thresholding to estimate fractions of granules containing one or both mucins. Plots of random continuous linear scans suggested granules containing only one mucin (open triangles) or both mucins (solid triangles) in airways stimulated with either IL-1β (Figures 3A and 3B) or IL-13 (Figures 3E and 3F). Segmentation by thresholding defined line segments within individual granules and determined whether both fluorophores or just one fluorophore was present in each intragranular segment (Figures 3C and 3G). Analysis of hundreds of granules from five mice showed similar results for the two cytokines (Figures 3D and 3H), with 41–43% of granules containing both mucins, 40–46% containing MUC5B alone, and only 12–15% containing MUC5AC alone. A small number of granules (1–2%) could not be categorized by our algorithm, which should not substantially affect the quantitative results.

In many cells, a rim of small granules containing only MUC5B was visible near the apical surface of cells stimulated with either cytokine (*see* Figures E3A and E3B). In occasional cells, the rim of small MUC5B granules surrounded a central region of MUC5AC granules, with a striking example imaged by confocal microscopy (*see* Figure E3C). The small MUC5B peripheral granules could represent hypothesized "constitutive-like" baseline secretory granules (35).

Colocalization of MUC5AC and MUC5B in Mouse Airways Stimulated with Elastase

To further assess colocalization of MUC5AC and MUC5B in mice, we used an additional model of mucous metaplasia induced by elastase instillation (36), together with high-resolution Airyscan imaging as explained in the Methods section of the online supplement (37). Antibody labeling of

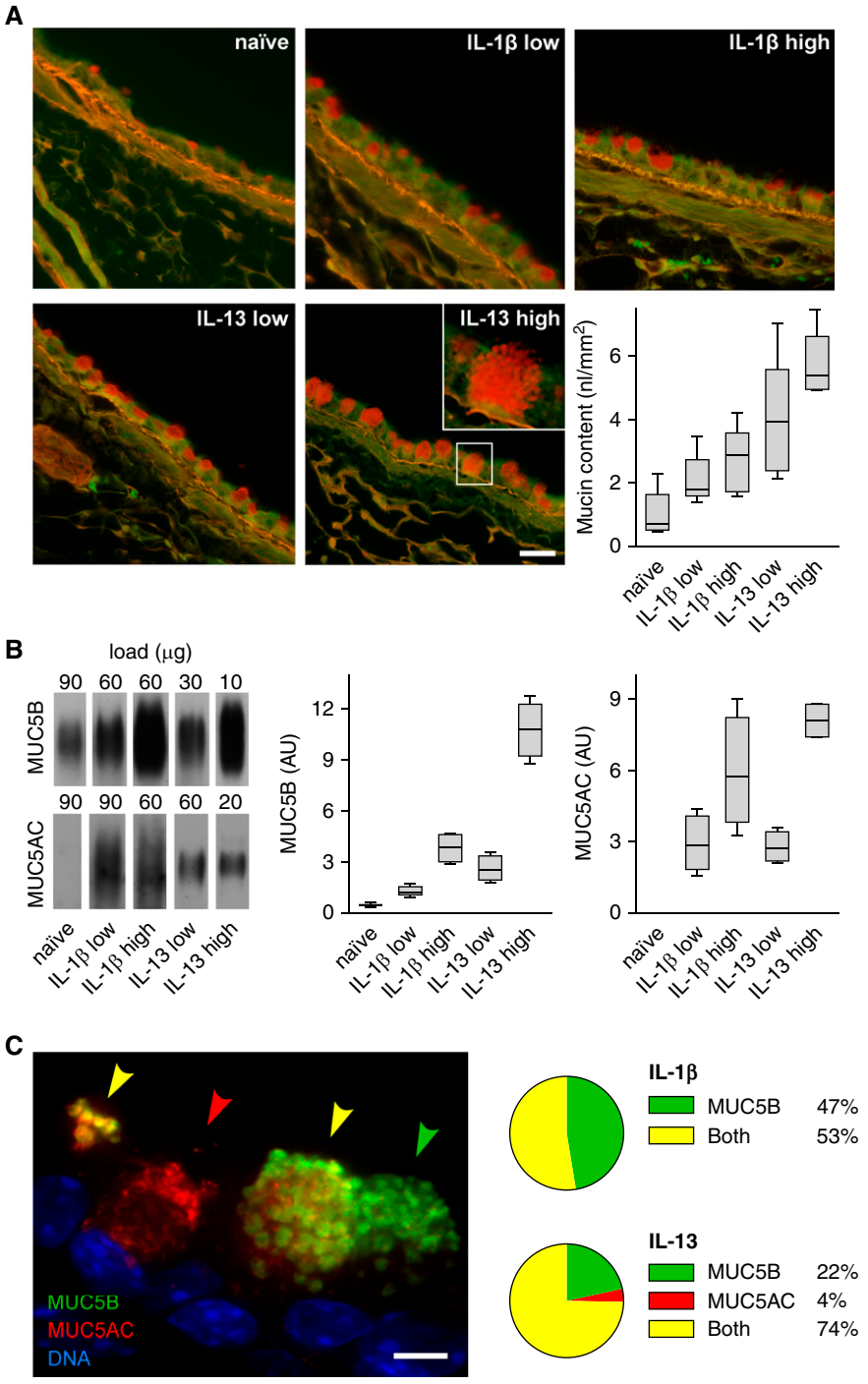

Figure 1. Mucin expression in mouse airways stimulated with cytokines. (*A*) Representative fields of periodic acid fluorescent Schiff (PAFS)-stained bronchial airways from naive (uninflamed) mice or mice stimulated with low or high doses of IL-1β or IL-13 to increase mucin production. Scale bars: main images, 25 μm; inset, 7 μm. Box plots show quantification of the intracellular mucin volume density (nl mucin/mm^2 basement membrane) in the left axial bronchus (boxes show median and interquartile range, and whiskers show fifth and 95th percentiles; for IL-1β low vs. IL-13 low, $P = 0.127$; for IL-1β high vs. IL-13 high, $P = 0.006$; $n = 5$ mice per group). (*B*) Representative immunoblots of right lung lysates from the same mice as in *A* probed for MUC5AC (mucin 5AC, oligomeric gel-forming) and MUC5B (mucin 5B, oligomeric gel-forming). The total protein loaded for each sample was different to avoid saturation. Box plots show densitometric analyses of the immunoblots derived from standard curves for each probe (for MUC5B, IL-1β low vs. IL-13 low, $P = 0.35$; for MUC5B, IL-1β high vs. IL-13 high, $P < 0.001$; for MUC5AC, IL-1β low vs. IL-13 low, $P = 0.99$; for MUC5AC, IL-1β high vs. IL-13 high, $P = 0.197$; $n = 5$ mice per group). (*C*) Image of a mouse airway after a low dose of IL-13 and stained with antibodies against MUC5AC (red) and MUC5B (green). Arrowheads indicate secretory cells containing MUC5AC only (red), MUC5B only (green), or both mucins (yellow). Scale bar, 5 μm. Pie charts indicate fraction of mucin-containing cells in the axial bronchus that have MUC5AC only, MUC5B only, or both mucins after a low dose of IL-1β (618 cells, four mice) or IL-13 (808 cells, four mice). Statistical comparison is provided in Figure E1 for this and all subsequent pie charts except Figures 4C and E9. AU = arbitrary units.

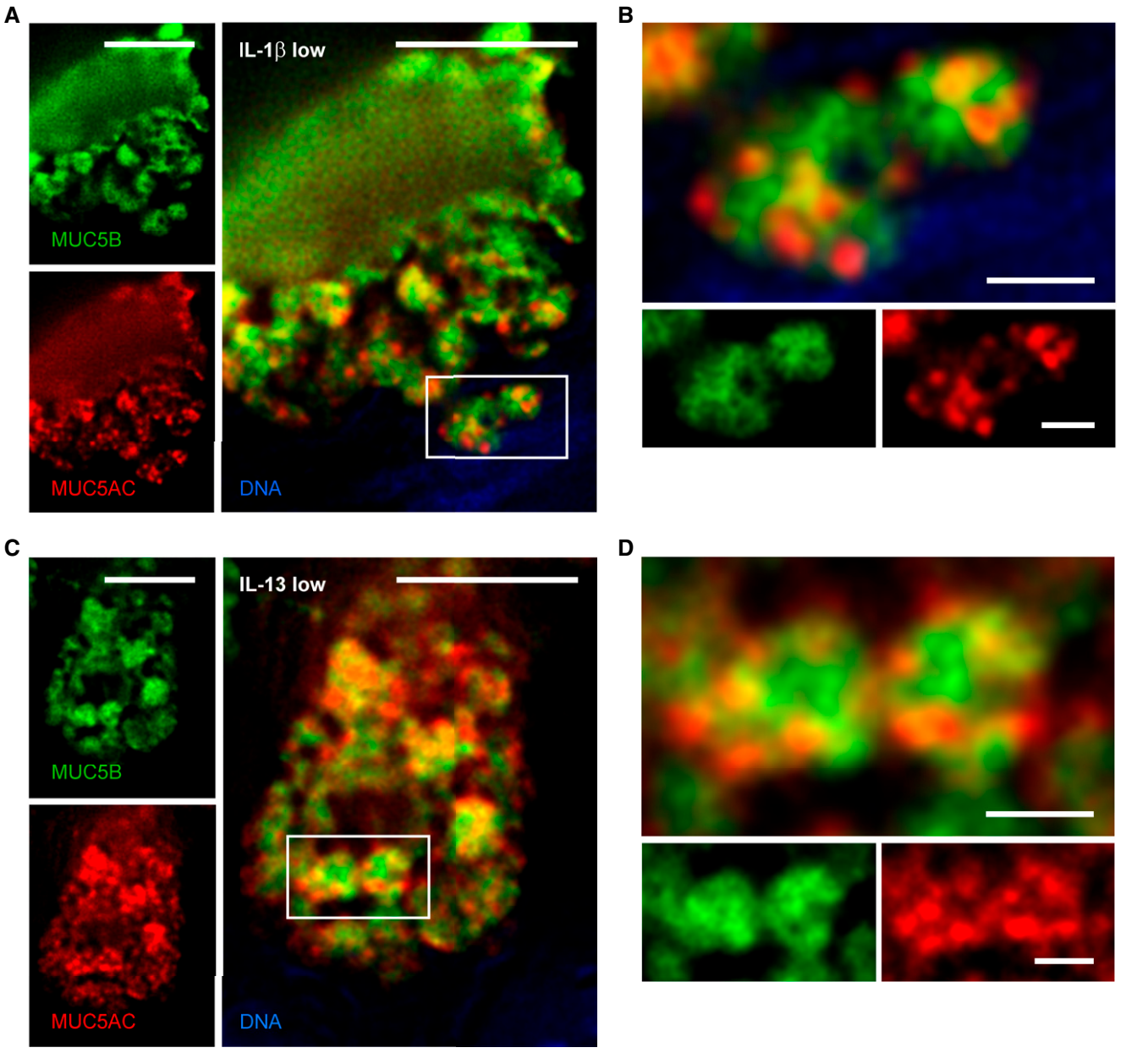

Figure 2. High-resolution deconvolution immunofluorescence microscopy of mucin granules in mouse airways stimulated with cytokines. (*A*) Deconvolved image of a mouse airway secretory cell after IL-1β challenge and staining with antibodies against MUC5AC (red) and MUC5B (green). Scale bar, 5 μm. (*B*) Higher magnification of mucin granules from box in *A* containing both mucins. Scale bar, 1 μm. (*C*) Image of a mouse airway secretory cell after IL-13 challenge and stained with the same antibodies. Scale bar, 5 μm. (*D*) Higher magnification of mucin granules from box in *C* containing both mucins. Scale bar, 1 μm. MUC5AC = mucin 5AC, oligomeric gel-forming; MUC5B = mucin 5B, oligomeric gel-forming.

mucins showed granules containing one or both mucins (Figure 4A), similar to cytokine-induced metaplasia (Figures 2 and 3). Line-plot profiles identified all three granule populations (Figure 4B; *see* additional examples in Figure E4). By object analysis, most granules contained both mucins, with only 16% containing MUC5B alone and 1% containing MUC5AC alone (Figure 4C; *see* Figure E5).

To corroborate the observations made with antibody staining, fluorescent tags were introduced by clustered regularly interspaced short palindromic repeats (CRISPR)/Cas methodology into the endogenous *Muc5b* (EGFP) and *Muc5ac* (mCherry) mucin genes (36). As for antibodies against MUC5AC (Figure 1), mCherry-MUC5AC was barely expressed in uninflamed mouse airways (not shown). To upregulate mCherry-MUC5AC, elastase was instilled into mCherry-MUC5AC/EGFP-MUC5B double-reporter mice, resulting in abundant mCherry-MUC5AC and EGFP-MUC5B expression

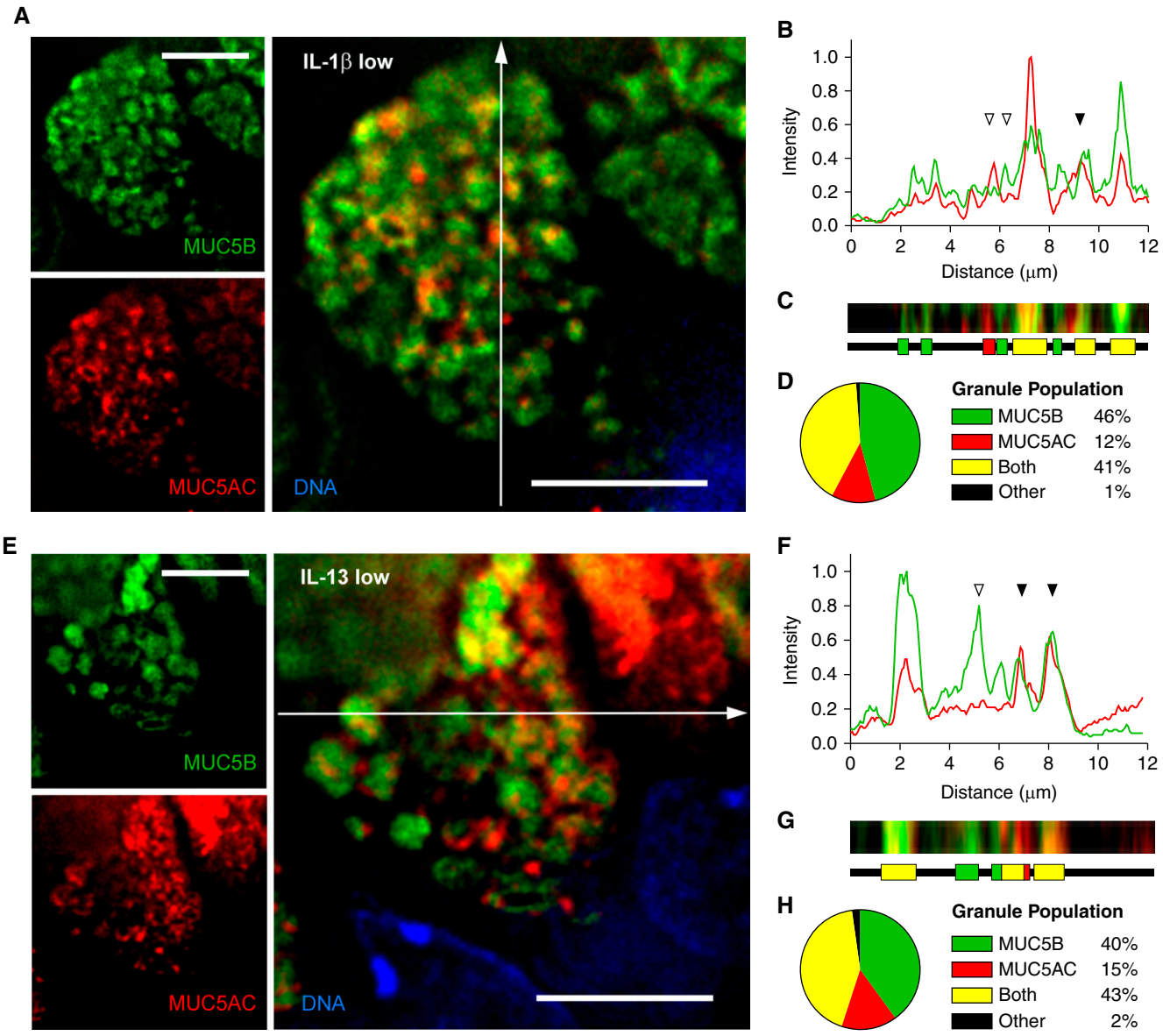

Figure 3. Quantitation of MUC5AC (mucin 5AC, oligomeric gel-forming) and MUC5B (mucin 5B, oligomeric gel-forming) colocalization within granules of mouse airways stimulated with cytokines. (*A* and *E*) Representative images of mouse airway secretory cells stimulated with IL-1β (*A*) or IL-13 (*E*), stained with antibodies against MUC5B (green) and MUC5AC (red), and imaged using deconvolution immunofluorescence microscopy. White lines indicate the area of measured pixel intensities plotted in *B* and *F*. Scale bar, 5 μm. (*B* and *F*) Line-scan analyses of pixels in the white lines in *A* and *E* are plotted as MUC5AC (red) and MUC5B (green) proportional fluorescence intensity (*y*-axis) versus the lengths of the white lines (*x*-axis). Fluorescence intensities were normalized for each image analyzed. Correspondence of the peaks for each line indicates colocalization of the mucins (solid triangles), whereas lack of correspondence indicates no colocalization (open triangles). (*C* and *G*) Color strips (top) correspond to the white lines but are three pixels wide and smoothed in Photoshop (Adobe) for visibility. Color ribbons (bottom) are generated after discarding the lowest third of pixel intensities in *B* and *F* to minimize background noise. Each color segment represents a counted granule. (*D* and *H*) Populations of all granules counted in the line-scan analyses. For IL-1β-treated mice: 730 granules, 83 cells, five mice; for IL-13 treated mice: 666 granules, 73 cells, five mice.

(Figure 4D). The presence of the three granule populations identified by immunofluorescence microscopy in cytokine- or elastase-stimulated wild-type airways were also observed in elastase-stimulated double-reporter mice (Figures 4C and 4D). At higher magnification, we again noted that the two mucins interdigitated within the granules (Figures 4E–4H; *see* Figure E6).

MUC5AC and MUC5B Expression in Human Airways

To determine whether mucins in human airways are packaged in a similar manner, we stained and analyzed human tissue as for

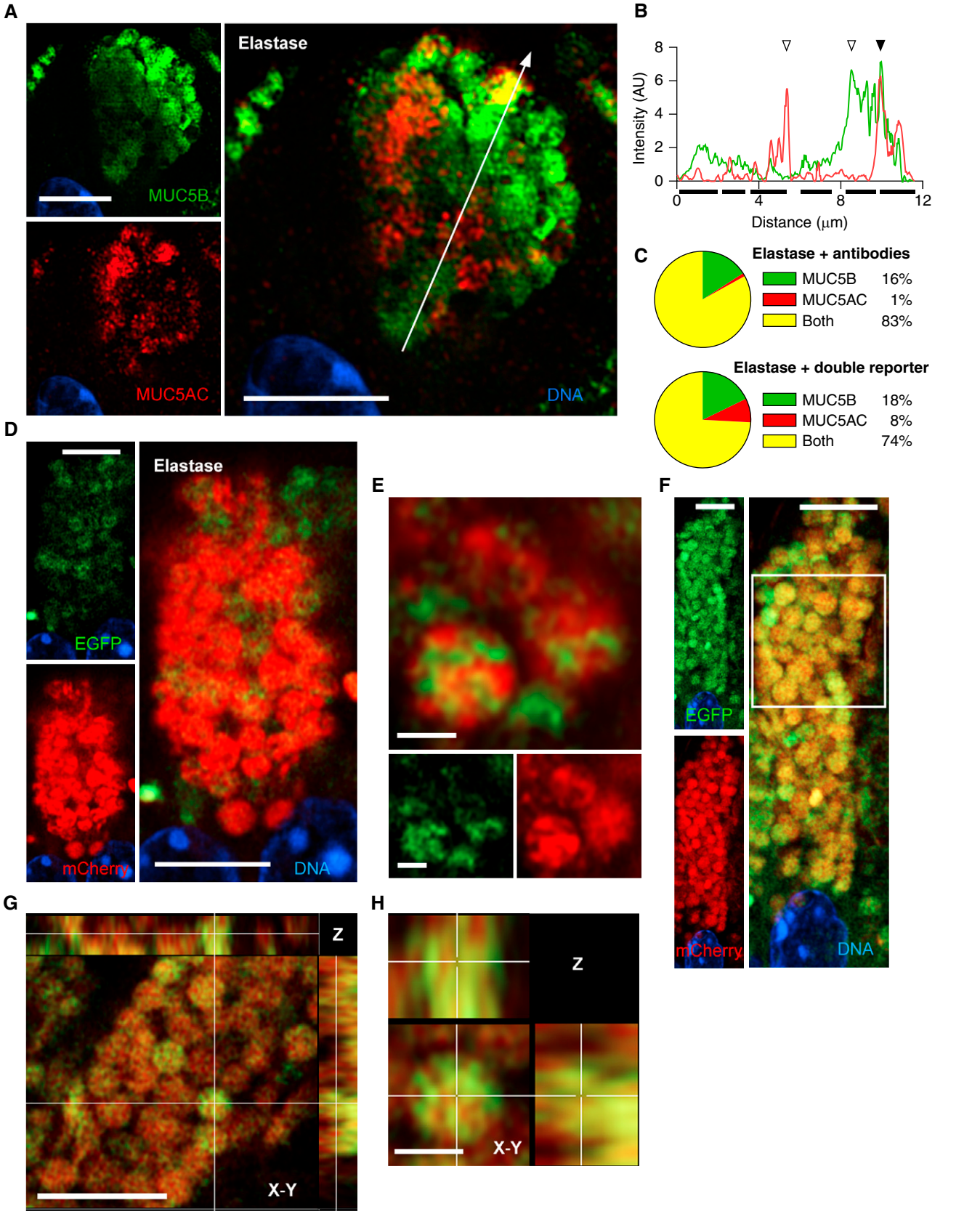

Figure 4. MUC5AC (mucin 5AC, oligomeric gel-forming) and MUC5B (mucin 5B, oligomeric gel-forming) colocalization in mouse airways stimulated with elastase. (*A*) Representative Airyscan image of a mouse airway secretory cell after elastase challenge and staining with antibodies against MUC5AC (red) and MUC5B (green). White line indicates the area of measured pixel intensities plotted in *B*. Scale bar, 5 μm.

mice, except that human airways were not stimulated with cytokines or elastase. Human tissue imaged in Figures 5–7 was nominally normal, obtained from lungs donated but not used for transplantation (*see* Table S1). However, some subjects had histories of cigarette smoking despite the absence of a diagnosed lung disease, and all subjects had been mechanically ventilated.

In human proximal airways (lobar and segmental bronchi), surface epithelial cells stained for both MUC5AC and MUC5B, whereas submucosal glands stained exclusively for MUC5B (Figure 5A). Mucus plaques adherent to the surface epithelium showed a heterogeneous mixture of MUC5AC and MUC5B (Figure 5A, white arrowhead). Luminal mucus emanating from the ducts of submucosal glands contained exclusively MUC5B in the distal region but was coated with MUC5AC proximally (Figure 5A, inset, yellow arrowhead), as has been observed for mucus emanating from the submucosal glands of pigs imaged with lectins (11, 12). Surface epithelial secretory cells in proximal human airways showed a higher fraction of cells containing both mucins or only MUC5AC (85% and 10%, respectively; Figure 5B) than did cells in the mouse axial bronchus stimulated with IL-1β (53% and 0%) or IL-13 (74% and 4%) (Figure 1C). Conversely, proximal human airways showed a much lower fraction of cells containing only MUC5B (5%; Figure 5B) than cells in the mouse axial bronchus stimulated with IL-1β (47%) or IL-13 (22%) (Figure 1C).

Surface epithelial cells in distal human airways (200–1,000 μm diameter) also were a mix of cells containing one or both mucins (Figure 5C). In distal airways that displayed longitudinal folds (Figure 5C), intracellular mucin content was higher at the base of furrows compared with the apex of ridges, as previously noted using histochemical stains (38). Most cells within individual folds contained predominantly the same mucin (Figure 5C). Similarly, in explants from subjects with chronic obstructive pulmonary disease (COPD) undergoing lung transplantation, the expression of MUC5AC and MUC5B tended to be locally uniform, though different airways within a single subject were highly variable (*see* Figure E7). Secretory cells in distal airways showed a distribution of cells containing one or both mucins similar to that in proximal airways, but with a higher fraction of cells expressing only MUC5B (5% in proximal vs. 19% in distal; Figure 5B), more closely resembling the mouse axial bronchus (Figure 1C). In further-distal airways with few mucin-containing cells, MUC5B expression predominated, but even in those cells, small amounts of MUC5AC were observed (Figure 5D). Granules in the most distal airways were noticeably smaller than those in more proximal airways.

Colocalization of MUC5AC and MUC5B within Mucin Granules in Human Airways

As for mouse airways, we focused on cells in human airways expressing both mucins and similarly observed granules containing one or both mucins (Figure 5; *see* Figure E7B). We again sought certainty that the fluorophores labeling each mucin were contained within a single granule using high-resolution widefield deconvolution microscopy. Similar to the results in mice, images of human proximal and distal airway secretory cells showed circular and elliptical regions filled by the two fluorophores, consistent with granules densely packed with mucins (Figure 6). Distal airway cells, in particular, showed interdigitating mucins that closely resembled mouse cells (Figure 6D). However, many granules in proximal airway cells showed small central regions devoid of fluorophores (Figure 6B, white arrowheads). Notably, mucin granules were spaced uniformly throughout the cytoplasm from the nucleus to the apical membrane, even in the tallest (~50 μm) proximal airway secretory cells (Figures 6A, 6C, 7A, and 7E; *see* Figures E8B and E8E), similar to the uniform spacing in mouse cells (Figures 3A, 3E, and 4F; *see* Figure E5).

Quantification of Mucin Granule Populations in Human Airways

To quantify the colocalization of MUC5AC and MUC5B, we performed widefield deconvolution immunofluorescence microscopy across numerous cells. Global statistical analysis by PCC yielded results similar to those for mice in both proximal (0.79; *see* Figure E2C) and distal (0.78; *see* Figure E2D) human airways. MCC analysis of human proximal airways (*see* Figure E2C) showed similar amounts of MUC5B colocalized with MUC5AC (M1 = 0.84) as MUC5AC colocalized with MUC5B (M2 = 0.82), resembling the patterns in cytokine-challenged mice (*see* Figures E2A and E2B). MCC analysis of human distal airways (*see* Figure E2D) yielded similar results (M1 = 0.79, M2 = 0.89).

The object-based analysis of segmentation by thresholding showed similar fractions of granules containing both mucins in human proximal (36%; Figure 7D) and distal (35%; Figure 7H) airways as in the axial bronchus of mice treated with IL-1β (41%; Figure 3D) or IL-13 (43%; Figure 3H). The fraction of granules containing only MUC5AC in human proximal (25%; Figure 7D) and distal (22%; Figure 7H) airways showed nonsignificant trends toward higher prevalence than in the axial bronchi of mice treated with IL-1β (12%; Figure 3D) or IL-13 (15%; Figure 3H), consistent with the higher expression of MUC5AC in human airways compared with mice (31). The fractions of granules containing only MUC5B were similar between human and mouse airways.

Colocalization of MUC5B and MUC5AC in Human Airways by Airyscan Microscopy

To further characterize mucin colocalization in human airways, tissue obtained by

Figure 4. (*Continued*). (*B*) Line-scan analysis of image in *A* is plotted as MUC5AC (red) and MUC5B (green) fluorescence intensity (*y*-axis) versus the length of the line (*x*-axis). Correspondence of the peaks for each line indicates colocalization of the mucins (solid triangles), whereas lack of correspondence indicates no colocalization (open triangles). Solid bars under the graph indicate individual granules. For additional examples, *see* Figure E4. (*C*) Populations of all granules counted in the line-scan analyses in samples stained with antibodies (top) or from reporter mice (bottom). Samples stained with antibodies: 440 granules, 44 cells, four mice; samples from reporter mice: 70 granules, seven cells, three mice; for samples stained with antibodies versus reporter mice, $P < 0.001$ by chi-square test. The complete data set of frequency distribution for granules imaged by immunofluorescence is shown in Figure E5. (*D*) Representative Airyscan image of an airway from a transgenic double-reporter mouse (EGFP-MUC5B/mCherry-MUC5AC) after elastase challenge. Scale bar, 5 μm. (*E*) High-magnification image of mucin granules from the same sample as *D*. Scale bars, 1 μm. (*F*) Another cell from a double-transgenic reporter mouse. White outline indicates area of higher magnification in *G*. Scale bar, 5 μm. (*G*) Higher magnification of the granules framed in *F* as well as the Z-plane reconstruction. Top panel, X-Z plane; right panel, Y-Z plane. Scale bar, 5 μm. (*H*) High magnification of a single granule from *G* showing X, Y, and Z planes. Scale bar, 1 μm. AU = arbitrary units; EGFP = enhanced green fluorescent protein.

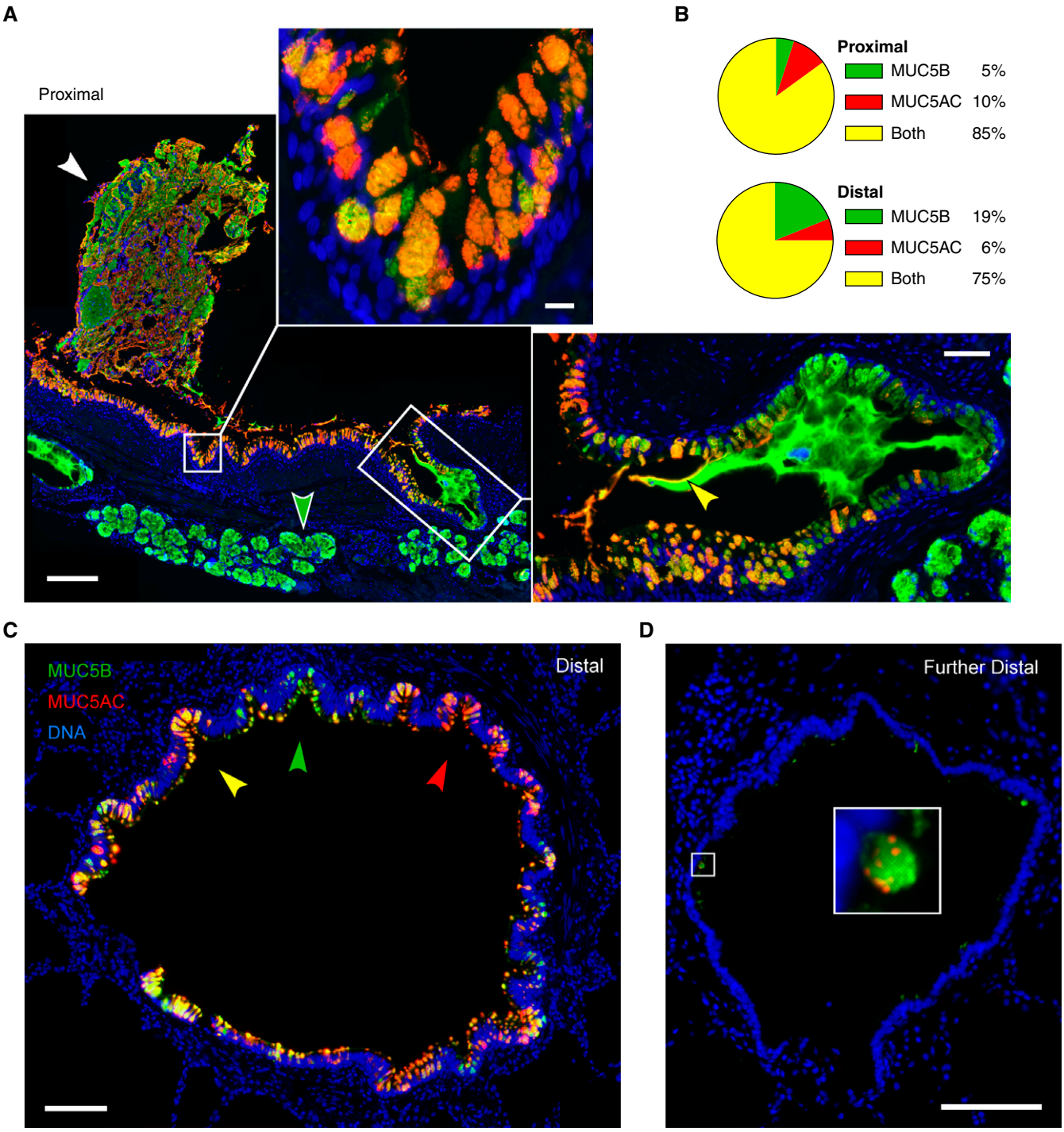

Figure 5. MUC5AC (mucin 5AC, oligomeric gel-forming) and MUC5B (mucin 5B, oligomeric gel-forming) expression in human airways. (*A*) Representative image of a human proximal airway stained with antibodies against MUC5AC (red) and MUC5B (green), depicting adherent mucus (white arrowhead), surface airway epithelium (top inset), and submucosal glands (green arrowhead and right inset). Scale bar, 200 μm. Top inset shows a higher magnification image of surface airway epithelium; scale bar, 10 μm. Right inset shows a submucosal gland duct opening into the airway with MUC5B-predominant luminal mucus and a thin coating of MUC5AC proximally (yellow arrowhead); scale bar, 50 μm. (*B*) Pie charts indicate fractions of mucin-containing cells in the proximal and distal airways that have MUC5AC only, MUC5B only, or both mucins. Proximal airways: 1,021 cells, eight subjects; distal airways: 1,687 cells, nine subjects. (*C*) Distal airway (~600 μm diameter) depicting furrows with epithelial cells containing predominantly MUC5AC (red arrowhead), MUC5B (green arrowhead), or both (yellow arrowhead). Scale bar, 100 μm. (*D*) A more distal airway (~400 μm diameter) containing little intracellular mucin but with scattered cells expressing both mucins. Scale bars: image, 100 μm; inset, 15 μm.

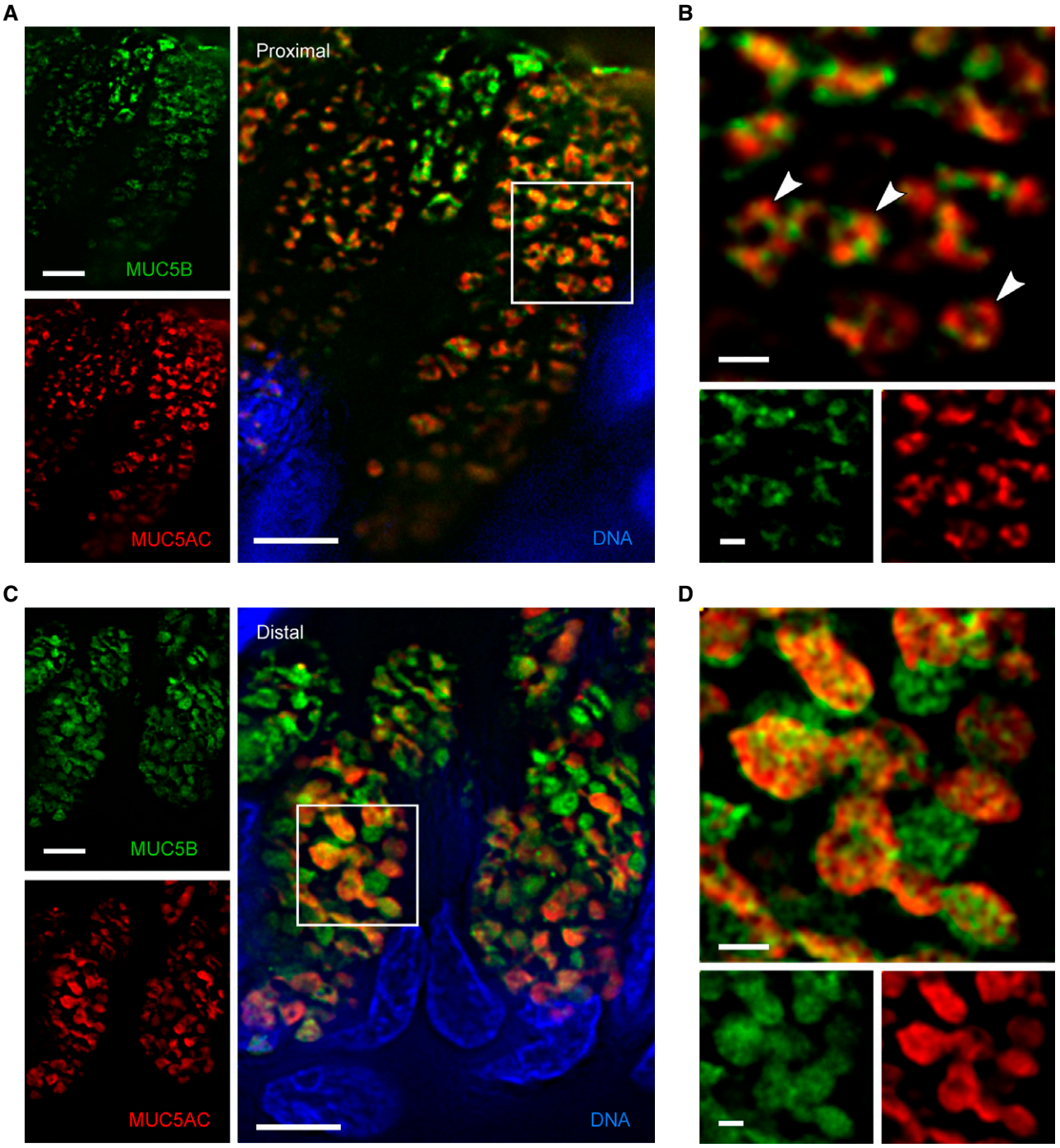

Figure 6. High-resolution deconvolution immunofluorescence microscopy of mucin granules in human airways. (*A*) Deconvolved image of secretory cells in a human proximal airway stained with antibodies against MUC5AC (red) and MUC5B (green). Scale bar, 5 μm. (*B*) Higher magnification of the boxed region in *A* showing mucin granules containing both mucins and a central lucency (white arrowheads). Scale bar, 1 μm. (*C*) Deconvolved image of secretory cells in a human distal airway stained with the same antibodies. Scale bar, 5 μm. (*D*) Higher magnification of the boxed region in *C*. Scale bar, 1 μm. MUC5AC = mucin 5AC, oligomeric gel-forming; MUC5B = mucin 5B, oligomeric gel-forming.

bronchoscopic biopsy of subjects with lung transplants was analyzed using Airyscan microscopy (Figure 8). Most of the cells containing both mucins showed them interdigitating within granules (Figures 8A–8C), similar to what was observed by deconvolution and Airyscan microscopy in mouse airways (Figures 2–4) and by deconvolution microscopy in human airways (Figures 5–7). However, occasional cells contained granules with MUC5B in the center surrounded by a rim of MUC5AC

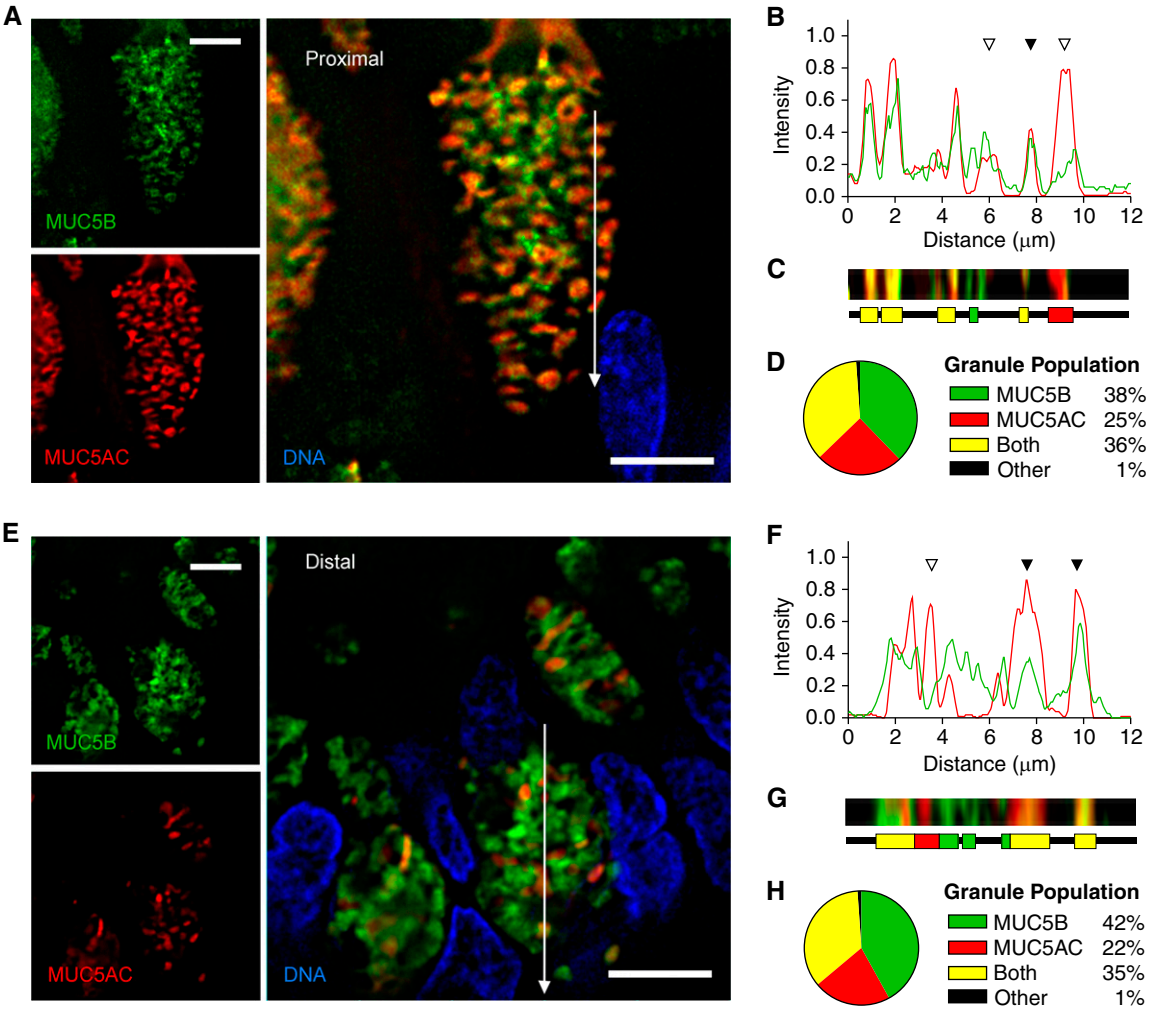

Figure 7. Quantitation of MUC5AC (mucin 5AC, oligomeric gel-forming) and MUC5B (mucin 5B, oligomeric gel-forming) colocalization within granules of human airways. (*A* and *E*) Representative deconvolved images of human proximal (*A*) and distal (*E*) airways stained with antibodies against MUC5AC (red) and MUC5B (green). White lines indicate the area of measured pixel intensities plotted in *B* and *F*. Scale bars, 5 μm. (*B* and *F*) Line-scan analyses of pixels in the white lines in *A* and *E* are plotted as MUC5AC (red) and MUC5B (green) proportional fluorescence intensity (*y*-axis) versus the lengths of the white lines (*x*-axis). Fluorescence intensities were normalized for each image. Correspondence of the peaks for each line indicates colocalization of the mucins (solid triangles), whereas lack of correspondence indicates no colocalization (open triangles). (*C* and *G*) Color strips (top) correspond to the white lines but are three pixels wide and smoothed in Photoshop (Adobe) for visibility. Color ribbons (bottom) are generated after discarding the lowest third of pixel intensities in *B* and *F* to minimize background noise. Each color segment represents a counted granule. (*D* and *H*) Populations of all granules counted in the line-scan analyses. For human proximal airways: 4,988 granules, 360 cells, eight subjects; for human distal airways: 1,138 granules, 106 cells, nine subjects.

(Figures 8D–8G). Detailed analysis of two such granules (α and β) at four different Z-planes showed peripheral MUC5AC, a mixed region (likely due to limited optical resolution), and a central MUC5B core (Figures 8F and 8G). To rule out the possibility that the segregation of the mucin isoforms might be due to an artifact of the differing wavelengths of the fluorophores on secondary antibodies, the fluorophores were switched, with the same outcome (*see* Figure E8). Such cells were also occasionally observed by widefield deconvolution microscopy in normal subjects (*see* Figure E8E).

Colocalization of MUC5AC and MUC5B in Cultured Human Airway Epithelial Cells

To further study the packaging of mucins within secretory granules, cultured airway epithelial cells could be valuable for live cell imaging, genetic manipulation, and other *in vitro* approaches. Therefore, we explored colocalization of MUC5AC and MUC5B in human proximal and distal airway cell cultures systems to determine whether they approximate findings in human airways *in situ*.

To model proximal airways, human airway epithelial cells (HAECs) were cultured at air–liquid interface in the presence or absence of IL-13 (*see* Figure E9). Without IL-13, 41% of cells expressed both mucins, and with IL-13, 31% expressed both mucins (*see* Figure E9C), compared with 85% expressing both mucins *in situ* (Figure 5B). As expected, without IL-13, a large fraction of cells expressed only MUC5B (42%),

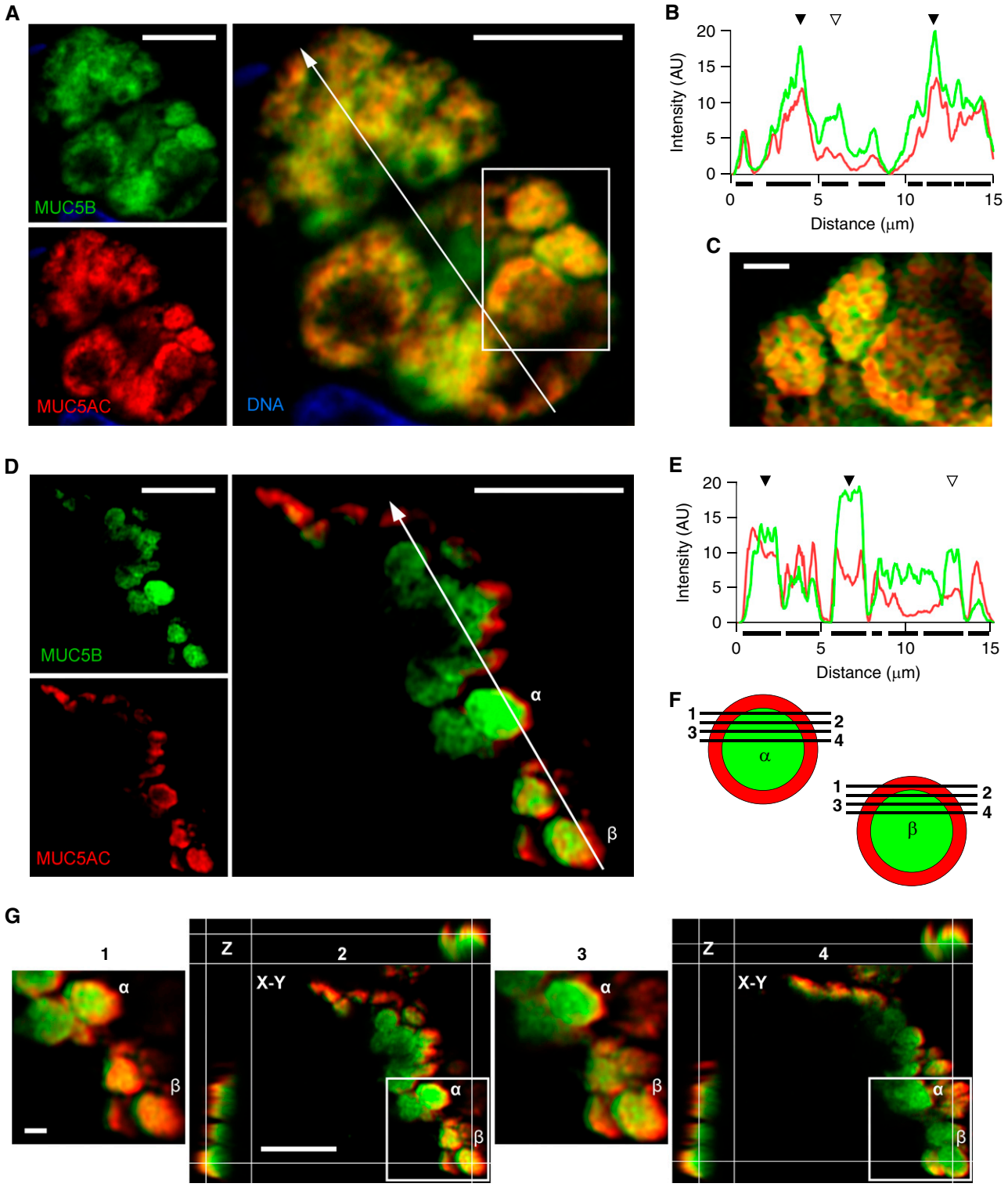

Figure 8. MUC5AC (mucin 5AC, oligomeric gel-forming) and MUC5B (mucin 5B, oligomeric gel-forming) colocalization in human airways imaged by Airyscan immunofluorescence microscopy. (*A*) Representative Airyscan image of a bronchial biopsy from a lung transplanted into a patient with cystic fibrosis, stained with antibodies against MUC5AC (red) and MUC5B (green). White line indicates the area of measured pixel intensities plotted in *B*. Scale bar, 5 μm. (*B*) Line-scan analysis of *A* is plotted as MUC5B (green) and MUC5AC (red) fluorescence intensity (*y*-axis) versus the length of the line (*x*-axis). Correspondence of the peaks for each line indicates colocalization of the mucins (solid triangles), whereas lack of correspondence indicates no colocalization (open triangles). Solid bars under the graph indicate localization of granules. (*C*) Higher magnification of mucin granules from box in *A* containing both mucins. Scale bar, 1 μm. (*D*) Representative Airyscan image of a

whereas with IL-13, a large fraction expressed only MUC5AC (62%). Consistent with the relatively low percentage of HAECs expressing both mucins, global statistical analyses (*see* Figure E9D) showed low PCC (0.30) and MCC (M1 = 0.31, M2 = 0.26) in the absence of IL-13, as well as its presence (PCC = 0.17) (MCC: M1 = 0.15, M2 = 0.28). Similarly, object-based analysis showed fewer granules in HAECs containing both mucins (without IL-13, 17%; with IL-13, 14%; *see* Figure E9G) than *in situ* (36%; Figure 7D).

To model distal airways, precision-cut lung slices (PCLS) harvested from the lung periphery were cultured (*see* Figure E10). For PCLS, 42% of cells expressed both mucins and 46% expressed only MUC5B (*see* Figure E10B), compared with cells *in situ*, of which 75% expressed both mucins and 19% expressed only MUC5B (Figure 5B). By object-based granule colocalization, 30% of granules contained both mucins and 46% contained only MUC5B with PCLS (*see* Figure E10F), compared with cells *in situ*, in which 35% of granules contained both mucins and 42% contained only MUC5B (Figure 7H). In summary, there are both similarities and differences between cultured and *in situ* cells that need to be considered when interpreting future imaging and functional studies in cultured cells.

Discussion

The production and secretion of polymeric mucins is an essential defense of the airways (1, 2, 18), and dysfunction of this process is central to multiple lung diseases. These include the muco-obstructive lung diseases asthma, COPD, cystic fibrosis, and bronchiectasis (4), as well as interstitial lung diseases (21). The muco-obstructive lung diseases are characterized by mucin hyperproduction, rapid secretion, and insufficient hydration, with mucus dysfunction most pathophysiologically significant in the extracellular airway lumen (1, 4, 24). This manifests as mucus plaque formation and luminal occlusion, resulting in inflammation, infection, and airflow obstruction. In the interstitial lung diseases, it is more likely that mucin hyperproduction causes cellular proteostasis stress resulting in lung epithelial progenitor depletion, though the pathophysiology is not yet certain (21, 22, 39, 40).

For all these diseases, it is critical to understand the intracellular trafficking of newly synthesized mucins and their packaging into secretory granules to allow insight into pathophysiologic mechanisms and the potential consequences of therapeutic targeting. To address these issues, we used high-resolution imaging of secretory cells in mouse and human airways. Our central findings are that most secretory granules in both mice and humans contain both mucins and that most commonly, the mucins interdigitate within the granules. The colocalization of both mucins within most granules makes it unlikely that the secretion of MUC5AC versus MUC5B can be differentially controlled as a therapeutic strategy to limit the presence of MUC5AC in luminal mucus, which can impair ciliary clearance (8, 41). Nonetheless, selective limitation of MUC5AC expression is being targeted with biologic agents directed at upstream mediators of allergic inflammation (42) and more directly by RNA interference (43). In addition, the efficacy of inhibiting rapid stimulated secretion of both mucins while preserving homeostatic baseline secretion has recently been validated in preclinical studies (27, 29, 44).

In focusing on cells in mice that contained both MUC5AC and MUC5B, we were able to observe the packaging of the two mucins within secretory granules by high-resolution widefield deconvolution immunofluorescence microscopy. This showed that most granules were almost completely occupied by the fluorochromes (Figure 2), suggesting that little or no material besides mucins was packaged within these granules. The dense interdigitation of MUC5AC and MUC5B within secretory granules was similarly observed in mice challenged with elastase and imaged using Airyscan immunofluorescence microscopy (Figure 4A) and in mucin-fluorescent protein chimeric double-reporter transgenic mice (Figures 4D–4H). The close interdigitation of the mucins in most granules suggests a stochastic packaging process in the trans-Golgi network, though ordered adjacent packing of MUC5AC and MUC5B is also possible. If packaging is ordered in some way and monitored by a cellular process, then proteostasis stress due to overexpression of MUC5B from the allele associated with idiopathic pulmonary fibrosis (45) might be sensed in the Golgi apparatus in addition to or instead of the endoplasmic reticulum (46, 47). The packaging of mucin species within secretory granules has been explored previously by biochemical and biophysical techniques (41, 48–51), and those results can now be integrated with our morphologic findings in further mechanistic studies.

Findings in proximal and distal human airways (Figures 5–8) were similar to those in mice (Figures 1–4), with some exceptions. First, mice required stimulation with cytokines to visualize MUC5AC, but humans did not. This probably reflects the fact that mouse proximal airways resemble human distal airways, with minimal MUC5AC expression in either in the absence of inflammation (31, 52). In addition, the mice we examined were only several weeks old and housed in protected environments, whereas the human subjects were exposed to environmental toxicants for decades, including cigarette smoke. Second, we observed in medium-sized human airways with prominent folds (Figure 5C), but not in mice, that secretory cells congregated at the base of furrows, as described previously (38), and that secretory cells within a single furrow tended to show the same pattern of expression of one or both mucins. We speculate that local interactions with immune cells or paracrine interactions among epithelial cells result in the relative homogeneity with furrows (53). Similarly, we observed local predominance of the expression of MUC5AC or MUC5B within individual airways of normal subjects and those with COPD but variable expression among different airways (*see* Figure E7). Third and similar to mice, most secretory granules in human airways showed dense interdigitation of MUC5AC

Figure 8. (*Continued*). bronchial biopsy from a lung transplanted into a patient with chronic obstructive pulmonary disease stained with the same antibodies. White line indicates the area of measured pixel intensities plotted in *E*. Two granules (α and β) are further analyzed in *F* and *G*. Scale bar, 5 μm. (*E*) Line-scan analysis of *D* is plotted as in *B*. Correspondence of the peaks for each line indicates colocalization of the mucins (solid triangles), whereas lack of correspondence indicates no colocalization (open triangles). (*F*) Schematic drawing of the separation of MUC5AC (red) and MUC5B (green) in the Z-plane (planes 1–4) of the two granules (α and β) in *D*. (*G*) Detailed analysis of the selected granules (α and β) at four different Z-planes (planes 1–4). Planes 2 and 4 show additional X-Z and Y-Z reconstruction. The granules show predominant MUC5AC staining (red) at their periphery and predominant MUC5B staining (green) in the center. Scale bar, 1 μm. AU = arbitrary units.

and MUC5B by immunofluorescence microscopy (Figures 6 and 7), though granules in proximal human airways often showed a nonfluorescent central region suggesting either that nonmucin molecules were packaged together with the mucins or that this region was not accessible to antibodies. Fourth, in the airways of human subjects who had undergone lung transplantation and were examined by transbronchial biopsy, granules containing an outer rim of MUC5AC surrounding a core of MUC5B were observed (Figures 8D–8G; *see* Figure E8D). Similar granules were occasionally observed in normal lungs (*see* Figure E8E) and in cells cultured from PCLS (*see* Figure E10C). Notably, this lamellar arrangement of mucins was observed exclusively in the most peripheral granules, suggesting that it may occur during exocytosis. Whether it reflects an artifact of fixation or a physiologic rearrangement of mucin polymers during secretion is not clear.

Our study has several limitations. Among these are the possibility that tissue handling during isolation and fixation could induce degranulation. However, the relatively uniform distribution of granules from apical to basal poles of most imaged human airway cells other than those obtained by bronchoscopic biopsy argues against this. Furthermore, the similarity in mucin packaging between mouse and human cells despite anatomic and metabolic differences between mice and humans suggests that we observed conserved features of mucin packaging. Another limitation is that we were unable to correlate the degree of cigarette smoke exposure with mucin expression and packaging, because of the limited information available about the human tissue specimens. A future systematic study that addressed these issues would be of interest.

Conclusions

We have evaluated the packaging of polymeric mucins within secretory granules of mouse airway secretory cells under carefully controlled conditions and in proximal and distal airways of human subjects with and without underlying lung diseases. We found that most surface airway secretory cells in mice and humans express both mucins and that most secretory granules contain both MUC5AC and MUC5B densely packaged in an interdigitating pattern. These observations can help guide further studies of intracellular mucin trafficking in unraveling the pathogenesis of multiple mucoobstructive and interstitial lung diseases and help in the design of therapeutic interventions in airway mucin production and secretion. ■

Author disclosures are available with the text of this article at www.atsjournals.org.

References

1. Fahy JV, Dickey BF. Airway mucus function and dysfunction. *N Engl J Med* 2010;363:2233–2247.
2. Knowles MR, Boucher RC. Mucus clearance as a primary innate defense mechanism for mammalian airways. *J Clin Invest* 2002;109:571–577.
3. Thornton DJ, Rousseau K, McGuckin MA. Structure and function of the polymeric mucins in airways mucus. *Annu Rev Physiol* 2008;70: 459–486.
4. Boucher RC. Muco-obstructive lung diseases. *N Engl J Med* 2019;380: 1941–1953.
5. Rose MC, Voynow JA. Respiratory tract mucin genes and mucin glycoproteins in health and disease. *Physiol Rev* 2006;86:245–278.
6. Kesimer M, Ford AA, Ceppe A, Radicioni G, Cao R, Davis CW, *et al.* Airway mucin concentration as a marker of chronic bronchitis. *N Engl J Med* 2017;377:911–922.
7. Kesimer M, Ehre C, Burns KA, Davis CW, Sheehan JK, Pickles RJ. Molecular organization of the mucins and glycocalyx underlying mucus transport over mucosal surfaces of the airways. *Mucosal Immunol* 2013; 6:379–392.
8. Bonser LR, Zlock L, Finkbeiner W, Erle DJ. Epithelial tethering of MUC5AC-rich mucus impairs mucociliary transport in asthma. *J Clin Invest* 2016;126:2367–2371.
9. Lachowicz-Scroggins ME, Yuan S, Kerr SC, Dunican EM, Yu M, Carrington SD, *et al.* Abnormalities in MUC5AC and MUC5B protein in airway mucus in asthma. *Am J Respir Crit Care Med* 2016;194: 1296–1299.
10. Ermund A, Meiss LN, Dolan B, Bähr A, Klymiuk N, Hansson GC. The mucus bundles responsible for airway cleaning are retained in cystic fibrosis and by cholinergic stimulation. *Eur Respir J* 2018;52:1800457.
11. Ostedgaard LS, Moninger TO, McMenimen JD, Sawin NM, Parker CP, Thornell IM, *et al.* Gel-forming mucins form distinct morphologic structures in airways. *Proc Natl Acad Sci U S A* 2017;114:6842–6847.
12. Ermund A, Meiss LN, Rodriguez-Pineiro AM, Bähr A, Nilsson HE, Trillo-Muyo S, *et al.* The normal trachea is cleaned by MUC5B mucin bundles from the submucosal glands coated with the MUC5AC mucin. *Biochem Biophys Res Commun* 2017;492:331–337.
13. Fakih D, Rodriguez-Piñeiro AM, Trillo-Muyo S, Evans CM, Ermund A, Hansson GC. Normal murine respiratory tract has its mucus concentrated in clouds based on the Muc5b mucin. *Am J Physiol Lung Cell Mol Physiol* 2020;318:L1270–L1279.
14. Fischer AJ, Pino-Argumedo MI, Hilkin BM, Shanrock CR, Gansemer ND, Chaly AL, *et al.* Mucus strands from submucosal glands initiate mucociliary transport of large particles. *JCI Insight* 2019;4: e124863.
15. Hasnain SZ, Evans CM, Roy M, Gallagher AL, Kindrachuk KN, Barron L, *et al.* Muc5ac: a critical component mediating the rejection of enteric nematodes. *J Exp Med* 2011;208:893–900.
16. Dickey BF. Exoskeletons and exhalation. *N Engl J Med* 2007;357: 2082–2084.
17. Campbell L, Hepworth MR, Whittingham-Dowd J, Thompson S, Bancroft AJ, Hayes KS, *et al.* ILC2s mediate systemic innate protection by priming mucus production at distal mucosal sites. *J Exp Med* 2019;216: 2714–2723.
18. Roy MG, Livraghi-Butrico A, Fletcher AA, McElwee MM, Evans SE, Boerner RM, *et al.* Muc5b is required for airway defence. *Nature* 2014; 505:412–416.
19. Costain G, Liu Z, Mennella V, Radicioni G, Goczi AN, Albulescu A, *et al.* Hereditary mucin deficiency caused by biallelic loss of function of *MUC5B. Am J Respir Crit Care Med* 2022;205:761–768.
20. Evans CM, Raclawska DS, Ttofali F, Liptzin DR, Fletcher AA, Harper DN, *et al.* The polymeric mucin Muc5ac is required for allergic airway hyperreactivity. *Nat Commun* 2015;6:6281.
21. Evans CM, Fingerlin TE, Schwarz MI, Lynch D, Kurche J, Warg L, *et al.* Idiopathic pulmonary fibrosis: a genetic disease that involves mucociliary dysfunction of the peripheral airways. *Physiol Rev* 2016;96: 1567–1591.
22. Dickey BF, Whitsett JA. Understanding interstitial lung disease: it's in the mucus. *Am J Respir Cell Mol Biol* 2017;57:12–14.
23. Livraghi-Butrico A, Grubb BR, Wilkinson KJ, Volmer AS, Burns KA, Evans CM, *et al.* Contribution of mucus concentration and secreted mucins Muc5ac and Muc5b to the pathogenesis of muco-obstructive lung disease. *Mucosal Immunol* 2017;10:395–407.
24. Jaramillo AM, Azzegagh Z, Tuvim MJ, Dickey BF. Airway mucin secretion. *Ann Am Thorac Soc* 2018;15:S164–S170.
25. Zhu Y, Ehre C, Abdullah LH, Sheehan JK, Roy M, Evans CM, *et al.* Munc13-2$^{-/-}$ baseline secretion defect reveals source of oligomeric mucins in mouse airways. *J Physiol* 2008;586:1977–1992.
26. Ren B, Azzegagh Z, Jaramillo AM, Zhu Y, Pardo-Saganta A, Bagirzadeh R, *et al.* SNAP23 is selectively expressed in airway secretory cells and mediates baseline and stimulated mucin secretion. *Biosci Rep* 2015; 35:e00220.

27. Jaramillo AM, Piccotti L, Velasco WV, Delgado ASH, Azzegagh Z, Chung F, *et al.* Different Munc18 proteins mediate baseline and stimulated airway mucin secretion. *JCI Insight* 2019;4:e124815.
28. Tuvim MJ, Mospan AR, Burns KA, Chua M, Mohler PJ, Melicoff E, *et al.* Synaptotagmin 2 couples mucin granule exocytosis to Ca^{2+} signaling from endoplasmic reticulum. *J Biol Chem* 2009;284:9781–9787.
29. Lai Y, Fois G, Flores JR, Tuvim MJ, Zhou Q, Yang K, *et al.* Inhibition of calcium-triggered secretion by hydrocarbon-stapled peptides. *Nature* 2022;603:949–956.
30. Evans CM, Williams OW, Tuvim MJ, Nigam R, Mixides GP, Blackburn MR, *et al.* Mucin is produced by clara cells in the proximal airways of antigen-challenged mice. *Am J Respir Cell Mol Biol* 2004;31:382–394.
31. Okuda K, Chen G, Subramani DB, Wolf M, Gilmore RC, Kato T, *et al.* Localization of secretory mucins MUC5AC and MUC5B in normal/healthy human airways. *Am J Respir Crit Care Med* 2019;199:715–727.
32. Hoang ON, Hales JB, Karmouty-Quintana H, Tuvim MJ, Dickey BF, Kurten RC. Mucin expression in human precision-cut lung slices [abstract]. *Am J Respir Crit Care Med* 2022;205:A5653.
33. Nguyen LP, Omoluabi O, Parra S, Frieske JM, Clement C, Ammar-Aouchiche Z, *et al.* Chronic exposure to beta-blockers attenuates inflammation and mucin content in a murine asthma model. *Am J Respir Cell Mol Biol* 2008;38:256–262.
34. Chen G, Sun L, Kato T, Okuda K, Martino MB, Abzhanova A, *et al.* IL-1β dominates the promucin secretory cytokine profile in cystic fibrosis. *J Clin Invest* 2019;129:4433–4450.
35. Davis CW, Dickey BF. Regulated airway goblet cell mucin secretion. *Annu Rev Physiol* 2008;70:487–512.
36. Fernández-Blanco JA, Fakih D, Arike L, Rodríguez-Piñeiro AM, Martínez-Abad B, Skansebo E, *et al.* Attached stratified mucus separates bacteria from the epithelial cells in COPD lungs. *JCI Insight* 2018;3:e120994.
37. Wu X, Hammer JA. ZEISS Airyscan: optimizing usage for fast, gentle, super-resolution imaging. *Methods Mol Biol* 2021;2304:111–130.
38. Quinton PM. Both ways at once: keeping small airways clean. *Physiology (Bethesda)* 2017;32:380–390.
39. Chen G, Ribeiro CMP, Sun L, Okuda K, Kato T, Gilmore RC, *et al.* XBP1S regulates MUC5B in a promoter variant-dependent pathway in idiopathic pulmonary fibrosis airway epithelia. *Am J Respir Crit Care Med* 2019;200:220–234.
40. Martino MB, Jones L, Brighton B, Ehre C, Abdulah L, Davis CW, *et al.* The ER stress transducer IRE1β is required for airway epithelial mucin production. *Mucosal Immunol* 2013;6:639–654.
41. Carpenter J, Wang Y, Gupta R, Li Y, Haridass P, Subramani DB, *et al.* Assembly and organization of the N-terminal region of mucin MUC5AC: indications for structural and functional distinction from MUC5B. *Proc Natl Acad Sci U S A* 2021;118:e2104490118.
42. Hammad H, Lambrecht BN. The basic immunology of asthma. *Cell* 2021;184:2521–2522.
43. Nicholas AS, Kasahara DI, Nguyen L, Trilling Z, Blanca-Afrazi M, Hamilton H, *et al.* Silencing Muc5ac expression with a lung-targeted RNAi trigger prevents allergen-induced mucoobstruction and airway hyperresponsiveness [abstract]. *Am J Respir Crit Care Med* 2022;205:A5491.
44. Gitlin I, Fahy JV. Mucus secretion blocked at its source in the lungs. *Nature* 2022;603:798–799.
45. Seibold MA, Wise AL, Speer MC, Steele MP, Brown KK, Loyd JE, *et al.* A common MUC5B promoter polymorphism and pulmonary fibrosis. *N Engl J Med* 2011;364:1503–1512.
46. López-Otín C, Blasco MA, Partridge L, Serrano M, Kroemer G. The hallmarks of aging. *Cell* 2013;153:1194–1217.
47. You K, Wang L, Chou CH, Liu K, Nakata T, Jaiswal A, *et al.* QRICH1 dictates the outcome of ER stress through transcriptional control of proteostasis. *Science* 2021;371:371.
48. Kesimer M, Makhov AM, Griffith JD, Verdugo P, Sheehan JK. Unpacking a gel-forming mucin: a view of MUC5B organization after granular release. *Am J Physiol Lung Cell Mol Physiol* 2010;298:L15–L22.
49. Ridley C, Kouvatsos N, Raynal BD, Howard M, Collins RF, Desseyn JL, *et al.* Assembly of the respiratory mucin MUC5B: a new model for a gel-forming mucin. *J Biol Chem* 2014;289:16409–16420.
50. Trillo-Muyo S, Nilsson HE, Recktenwald CV, Ermund A, Ridley C, Meiss LN, *et al.* Granule-stored MUC5B mucins are packed by the non-covalent formation of N-terminal head-to-head tetramers. *J Biol Chem* 2018;293:5746–5754.
51. Perez-Vilar J, Hill RL. The structure and assembly of secreted mucins. *J Biol Chem* 1999;274:31751–31754.
52. Young HW, Williams OW, Chandra D, Bellinghausen LK, Pérez G, Suárez A, *et al.* Central role of Muc5ac expression in mucous metaplasia and its regulation by conserved 5′ elements. *Am J Respir Cell Mol Biol* 2007;37:273–290.
53. Johnston SL, Goldblatt DL, Evans SE, Tuvim MJ, Dickey BF. Airway epithelial innate immunity. *Front Physiol* 2021;12:749077.